XVI. INTERACTION OF LASER RADIATION WITH PLASMAS AND NONADIABATIC MOTION OF PARTICLES IN MAGNETIC FIELDS*

Academic and Research Staff

Prof. D. J. Rose
Prof. T. H. Dupree
Prof. L. M. Lidsky

Graduate Students

T. S. Brown
J. D. Callen
J. F. Clarke
D. E. Crane
W. T. Hebel
M. D. Lubin
R. W. Moir
A. A. Offenberger
M. A. Samis

A. LASER RADIATION THOMSON-SCATTERED BY AN ELECTRON BEAM

The experiment described in Quarterly Progress Report No. 79 (pages 143-144) has been completed and the results are summarized in this report.

The purpose of the experiment was to experimentally verify the derived relationship among the angle that the electron beam makes with the observation direction, the velocity of the electrons, and the shift in wavelength of the laser radiation. The components involved in the experiment were completed. The observation system was scanned from 6700 Å to 6800 Å. The angle of observation was varied from 110° to 125°, and the voltage was varied from 800 volts to 1100 volts. The experiment was done by first setting a voltage and angle for the electron beam, making a rough calculation of the position of the shifted wavelength, then scanning the interference filter over the scattered signal envelope in 2.5 Å steps. The signal amplitude was recorded at each wavelength and the wavelength of the center of the envelope was taken to be the scattered wavelength. The results agreed within 1 Å (in 150 Å) with the theoretical predictions, which gives evidence of the correctness of the theoretical transformation equation. Also, the amplitude of the scattered signal agreed with the calculated value. The experiment is discussed more fully in the author's S.M. thesis entitled "Study of Laser Radiation Thomson-Scattered by an Electron Beam," conducted in the Department of Nuclear Engineering and the Research Laboratory of Electronics of the Massachusetts Institute of Technology.

M. A. Samis

B. NONADIABATIC TRAPPING EXPERIMENT

1. Resonant-Particle Measurements

During the past quarter, considerable progress has been made in determining the modes of particle escape from the nonadiabatic trap described in Quarterly Progress Report No. 81 (pages 141-147). A new diagnostic, that of ion collection, has been added,

*This work was supported by the United States Atomic Energy Commission (Contract AT(30-1)-3285).

and the problems of detector sensitivity mentioned in the last report have been solved by the development of a fast low-noise miniaturized preamplifier. A new 15-period corkscrew having a maximum perturbing field of 2 per cent was also installed. Figure XVI-6 shows the method of construction and illustrates schematically the changing pitch of the conductors. Because of the large number of periods in this corkscrew, some of the current windings were very closely packed. We found that displacements of the conductors by as little as their own diameter had an appreciable effect (~10%) on the local corkscrew field. As a result, any movement of the corkscrew windings in the course of the experiment produced small (less than 10%) changes in the quantities under investigation. Qualitatively, however, the results obtained were insensitive to these small changes in the perturbation.

Figure XVI-1 shows the measured amount of perpendicular energy possessed by the beam at the end of its initial transit through the corkscrew as a function of the helix current. With a 5:1 mirror ratio, $v_\perp^2/v^2 = 0.20$ is sufficient to trap the beam. With the mirrors turned on, the beam was pulsed, and the decay of the trapped particles through the end mirror was measured.

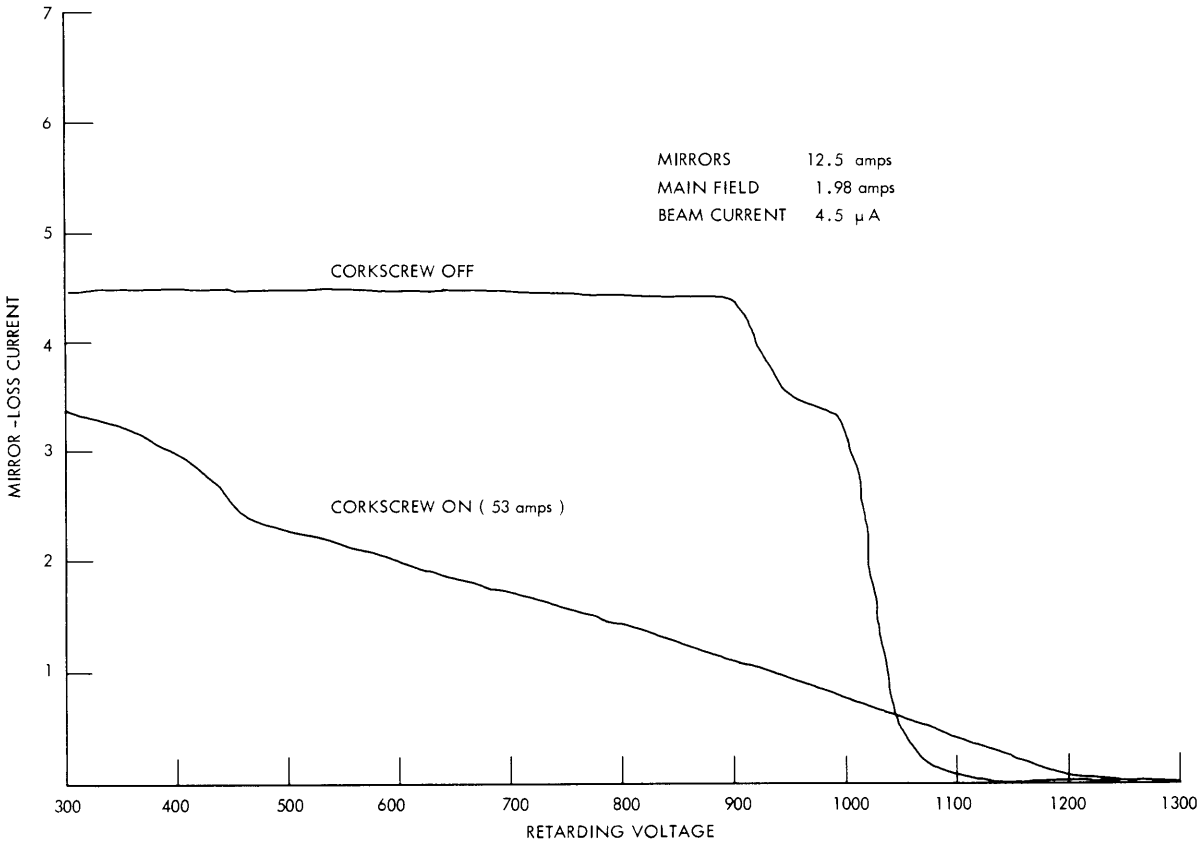

Fig. XVI-1. Magnetic moment after first transit.

Figure XVI-2 shows the decay curves obtained for three filling pulses. The rapid initial decay has a time constant of approximately 2 μsec, independent of the length of the filling pulse. The time constants of the long-lived tails, on the other hand, increase as a function of pulse length. Also, integration of these decay curves shows that the fraction of trapped particles associated with the long-lived tails also increases with pulse length.

The value of the short decay constant can be obtained by associating the rapid initial particle loss with the preferential downward scattering[1] in that region of velocity space where particles can resonate with the corkscrew. The value of the long decay constant can be obtained by associating the long-lived particles with those scattered into and out of the region of velocity space above the resonant region.

The increase of the time constant and the number trapped in this long-lived group with increasing pulse length is then due to the fact that as the filling pulse lengthens, particles have time to diffuse farther and farther into the nonresonant region. No equilibrium is achieved here, because the diffusion coefficient drops so rapidly away from resonance.[2] Since the resonant region lies closer to the loss cone, all particles must exit by way of preferential downward scattering. Thus, when the beam is turned off, we see, first, a rapid decay of those particles in the resonant region, followed by the exit of the particles stored in the diffusive group.

Energy analysis of the escaping particles[1] confirms that they are scattered out in the large steps produced by resonance. This effect is especially pronounced in the case shown in Fig. XVI-3. Here a partially wound 1600 V-beam is injected into the trap. The top trace shows the energy analysis of the beam with no corkscrew current. The beam is double peaked; the data show that in the uniform field region of the device, the two components had 7 per cent and 8 per cent of their main magnetic field. When the corkscrew is energized, the beam is trapped and the escaping particles are energy analyzed in the lower trace. It is clear that the resonant scattering has given the escaping particles more parallel energy that the injected beam possessed.

Figure XVI-4 shows the energy analysis when the injected beam is adjusted to resonance with the entrance conditions of the corkscrew. This is the condition for maximum initial trapping and longest lifetime of the trapped particles.[1] The almost linear slope on the lower curve shows that under optimum trapping conditions the escaping particles fill the loss cone of velocity space almost uniformly.

The picture of field-particle scattering in tuned helical nonadiabatic traps that has emerged from these experiments is shown schematically in Fig. XVI-5. The trapping resonance is the largest possible scattering that the particle can experience. It places the injected beam somewhere between the dotted lines in the diagrams, the location depending on the precise adjustment of the main field, the beam energy, the beam energy distribution, and the corkscrew current. On the second forward transit, the trapped

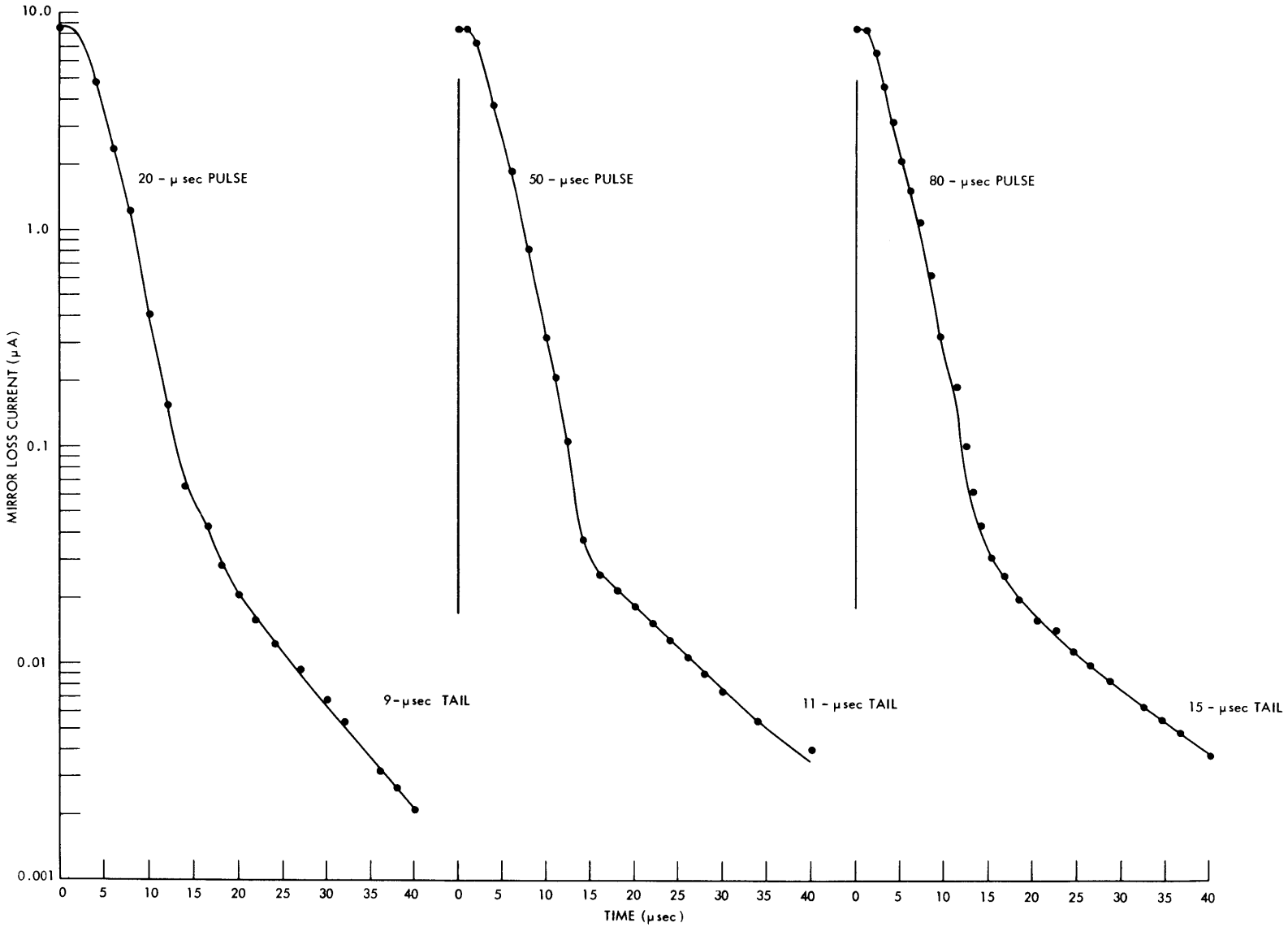

Fig. XVI-2. Variation of lifetime with pulse length.

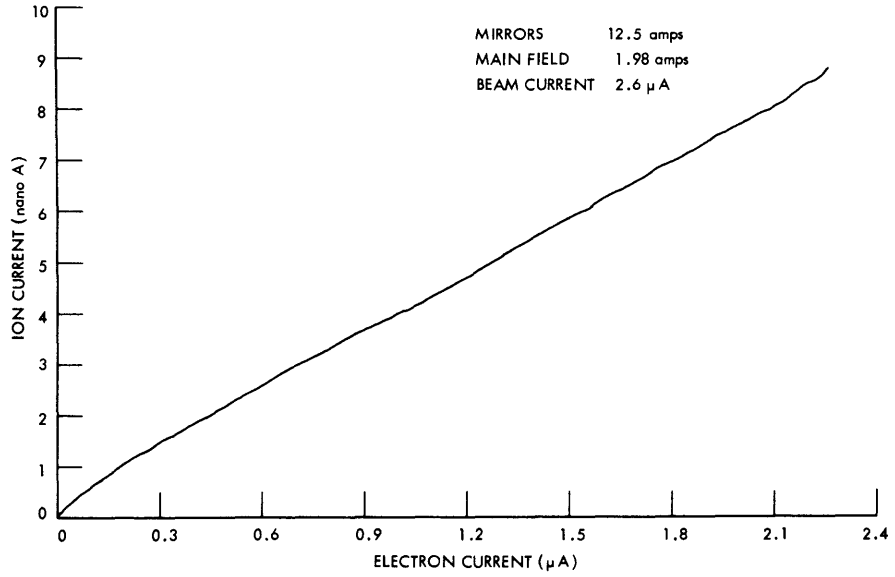

Fig. XVI-3. Energy distribution in the magnetic mirror.

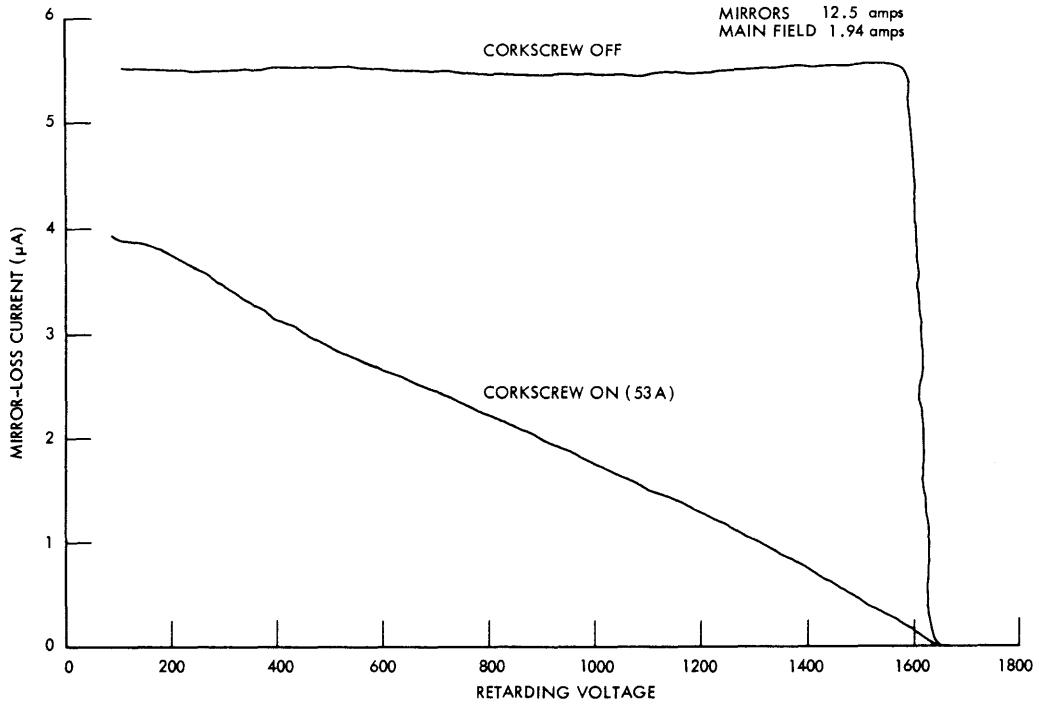

Fig. XVI-4. Energy distribution in the magnetic mirror.

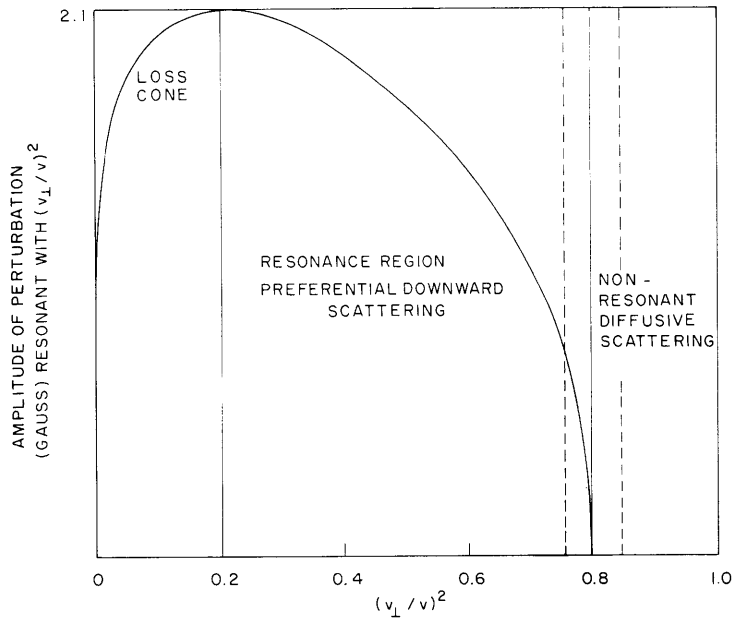

Fig. XVI-5. Summary of particle-corkscrew interaction.

particles that have an essentially random phase distribution are scattered either farther away from or back into the resonance region on the third transit. Because of the damping of the perturbation field those particles scattered downward on the second transit are resonantly scattered in a stronger field, make a larger downward step, and are rapidly lost. Those particles scattered away from resonance on the second transit interact with a weak nonresonant field and experience a small-step diffusive scattering with a lifetime that increases if they diffuse further from resonance. Unfortunately, from the viewpoint of trapping, this diffuse group is fed by only a small part of the injected beam. The existence of preferential downward scattering on the second transit insures that most of the beam scatters downward into the resonance region. The best measurement, thus far, shows 23 per cent of the total trapped particles in this diffusive group with a lifetime of approximately 11 μsec. With 77 per cent of the trapped particles in the resonant scattered group with a lifetime of approximately 2 μsec, the trap is operating at approximately 2 per cent efficiency as compared with the Liouville limit set by the experimental injected beam density.

2. Ion Detection

Figure XVI-6 shows the ion collector used in the experiment. In operation ions produced by electrons within the volume defined by the inner screen are trapped by this screen's -3 volt bias. Gas scattering eventually delivers a proportion of these ions to the collector that is biased at -300 volts, both to aid in the ion-collection efficiency and

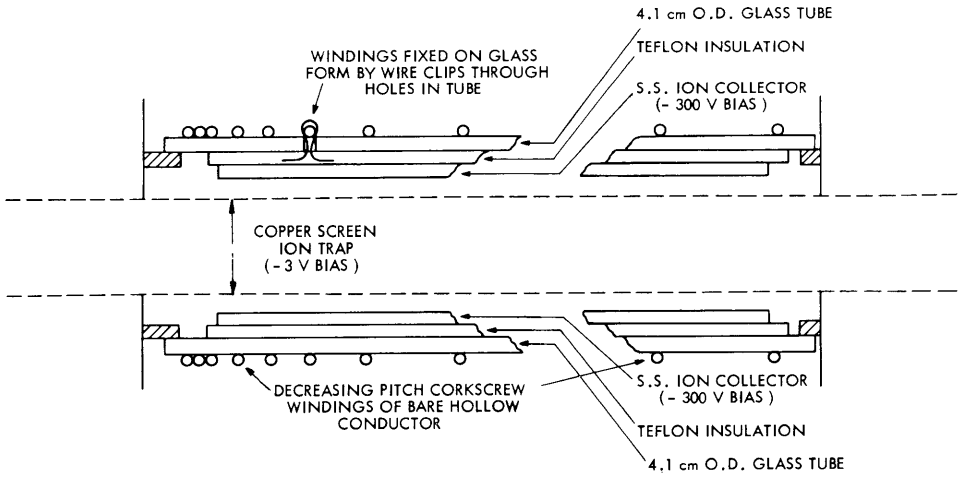

Fig. XVI-6. Ion collector and corkscrew assembly.

to repel secondary electrons. Particles whose orbits are the tightest spirals spend less time in mirror reflection and consequently make more ions within the collector per second. These particles constitute the long-lived diffusive group mentioned above. Thus lifetimes derived from ion-current measurements serve as upper limits to particle-confinement times, and it is difficult to gather more detailed information without knowledge of the distribution within the trap.

Another disadvantage of this technique is that it is very sensitive to the presence of secondary electrons produced by the injected beam when it strikes any material surface. These secondary electrons are mainly of low energy; consequently, their collision cross section with gas molecules is quite high, yielding an ion current out of proportion to their number. We have attempted to minimize this difficulty by using efficient beam collection outside the mirrors and eliminating high secondary emission coefficient materials within the trap. In spite of these limitations, ion collection has the advantage of the high accuracy of DC measurements, and constitutes a small perturbation probe of conditions within the trap.

The ion current is related to the trapped electrons by simple balance conditions. The time rate of change of the number of trapped particles, N_T, is

$$\frac{dN_T}{dt} = \frac{I_-}{q}\left(f + \frac{\tau}{\tau_g}\frac{A_T}{A}\right) - \frac{A_L}{A}\frac{N_T}{\tau_g} - \frac{N_T}{\tau_H} \tag{1}$$

where I_- is the injected beam, f is the fraction of the beam trapped by the initial corkscrew resonance, and τ, τ_g, and τ_H are the transit, gas-scattering, and helix-decay times, respectively. The A_T, A_L refer to the areas on the velocity surface of area A where particles are trapped by the magnetic mirrors or lost through the mirrors. Since

gas scattering is assumed to be isotropic in velocity space, a scattered particle has equal probability of landing anywhere on the velocity surface. Since the area associated with the loss cone is smaller than the total area, the probability of scattering out of the trap is reduced by A_L/A. Similarly, the probability of scattering into the trapped region is reduced by A_T/A. The ion-balance equation is

$$\frac{dN_+}{dt} = \frac{N_T}{\tau_+} - \frac{I_+}{q}, \tag{2}$$

where I_+ is the collected ion current, and τ_+ is the ionization time. In the steady state we have

$$I_+ = \frac{I_-}{\tau_+} \frac{f + \frac{\tau}{\tau_g}\frac{A_T}{A}}{\frac{1}{\tau_H} + \frac{A_L}{A}\frac{1}{\tau_g}} \tag{3}$$

With no corkscrew

$$I_+ = I\left(\frac{\tau}{\tau_+}\right)\frac{A_T}{A_L}. \tag{4}$$

Notice that the ion current is larger than one would expect on the basis of the beam alone. The factor (A_T/A_L) is due to the gas trapping of particles scattered out of the beam on its passage through one mirror and out of the other. When the corkscrew is turned on, we have

$$I_+ = I_- f \frac{\tau_H}{\tau_+} \tag{5}$$

under the assumption that $\tau A_T/A\tau_g \ll 1$ and $\tau_H < \frac{A}{A_L}\tau_g$, which is certainly true for a 5:1 mirror ratio, where $A_T/A = 0.9$ and $A/A_L = 10$. Taking the ratio of Eq. 5 to Eq. 4, we get

$$\frac{I_+ \text{ (helix on)}}{I_+ \text{ (helix off)}} = \frac{A_L}{A_T}\frac{f\tau_H}{\tau}. \tag{6}$$

Figure XVI-7 shows an experimental measurement of I_+ as a function of helix current. The rise in I_+ at 32.5 amps corresponds to the measurement of wind-up as a function of helix current from retarding potential measurements shown in Fig. XVI-1. The critical nature of the adjustment to obtain the best trapping is illustrated by the narrowness of the peak. At the peak we can assume that $f = 1$ and obtain an estimate of particle lifetime in the trap.

$$\tau_H = \left(\frac{A_T}{A_L}\right) \frac{I_+ \text{ (helix on)}}{I_+ \text{ (helix off)}} \tau,$$

and

$$\tau_H = 18.2 \ \mu\text{sec}.$$

This is quite consistent as an upper limit on the long-lived group decay measured by the pulse technique. Because the function f is unknown away from the peak, this lifetime

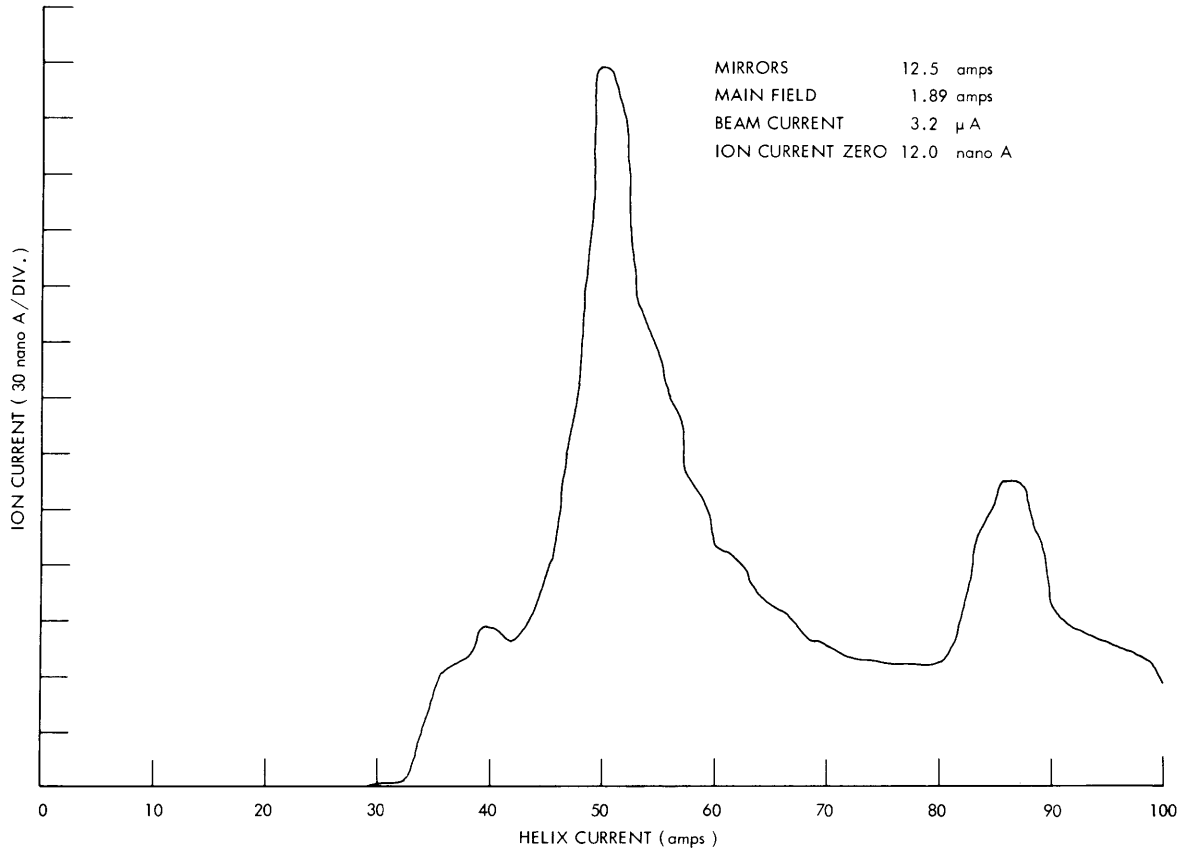

Fig. XVI-7. Ion current produced by corkscrew trapped particles.

estimate is the only piece of quantitative information obtainable from curves such as are shown in Fig. XVI-7; however, the adjustment of the system parameters for optimum trapping is indicated by the peak in such a trace and this was used an an optimizing criterion for the pulse measurments.

The second peak in Fig. XVI-8 shows that trapping occurs for currents higher than the corkscrew design current. This is due to the design equations for the corkscrew field which require

$$I_o \cos \chi_o = \text{constant},$$

where I_o is the helix current, and χ_o is the field-particle phase of a particle in the design orbit. As I_o increases the design orbit shifts toward $\chi_o = \pi/2$. Since the beam is adjusted for a specific entrance phase, increasing I_o shifts the beam into an unstable orbit. For sufficiently high currents, the unstable beam particle can be wound up and completely unwound in the first few turns of the corkscrew. The phase of these unwound particles is indeterminate. A simple consideration of the forces on the unwound particle shows, however, that it takes up a phase near $\pi/2$. This is near the phase of the design orbit, and the beam can be wound up again.

3. "Dissociation" Experiment

We have shown that the dominant loss mechanism for particles that have been trapped by means of a resonant nonadiabatic perturbation is the resonant scattering occurring when a trapped particle experiences a local resonance with the perturbation. It has been suggested[3, 4] that one can avoid this loss by dissociating the injected particles so that they can no longer satisfy the resonance relation

$$v_{||} = \frac{qB_o p(z)}{2\pi m}, \tag{7}$$

where p(z) is the varying pitch of the perturbation super-imposed on a uniform field, B_o.

For molecular ion injection, the velocity of the dissociated ion is the same as that of the injected molecule, but its mass is decreased by half. Thus for this particle, Eq. 7 becomes an inequality,

$$v_{||} < \frac{qB_o p(z)}{2\pi(m/2)}, \tag{8}$$

and no local resonance is possible. Notice that Eq. 8 can be rewritten

$$v_{||} < \frac{q(2B_o)\, p(z)}{2\pi m}. \tag{9}$$

Now, if we design a corkscrew (that is, specify p(z)) to trap a particle of velocity v and mass m in a magnetic field B_o, and then study the interaction of the same particle with the corkscrew in a field $2B_o$, Eqs. 8 and 9 tell us that we are studying the dissociated-particle interaction. Figure XVI-8 shows the situation in velocity space with a loss cone equal to that in our experiment. In a full-scale injection experiment, molecular ions of mass 2m and velocity v/2 are trapped by a resonance on the inner velocity surface. Dissociated ions will remain on the same velocity surface, but since their mass is decreased by two, their resonance region is located on the outer surface in this figure.

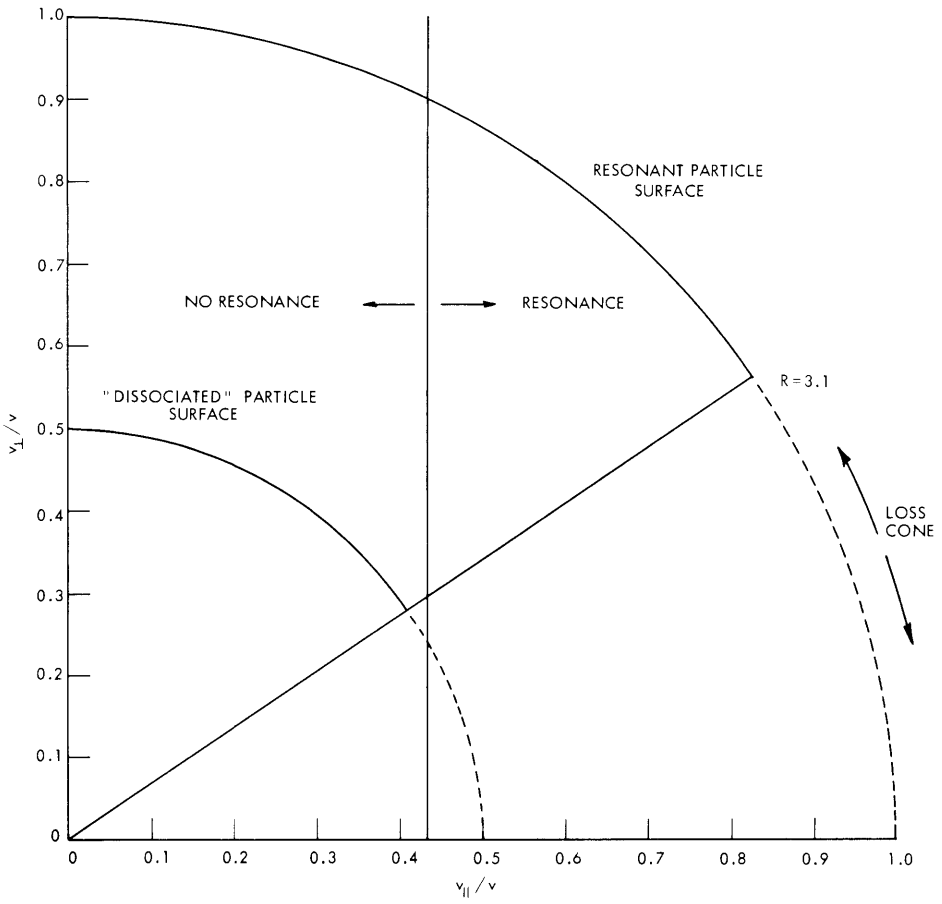

Fig. XVI-8. Velocity-space diagram of "dissociated" particle experiment.

In our experiment we can study the escape of these dissociated particles in a particularly simple fashion. We adjust the apparatus so that the trapping resonance lies on the outer surface of Fig. XVI-8 and inject a beam of electrons with $v_\parallel/v = 1/2$ and $v_\perp/v = 0$. Since these electrons are on the inner velocity surface, they cannot be trapped by the corkscrew resonance; however, while they pass through the region between two magnetic mirrors, gas scattering will trap some of them. In other words, gas scattering will populate the inner velocity surface with a low density of electrons. We can then study the nonresonant effects of the perturbation on these particles. Because the surface is thinly populated in a continuous fashion and the perturbation will cause only a small change in the gas-scattering equilibruim, the sensitive ion-collection technique was chosen as the initial diagnostic.

Figure XVI-9 shows a measurement of ion current as a function of electron beam current with no corkscrew. The linearity of the curve is predicted by Eq. 4 as

$$I_+ = \left(\frac{A_T}{A_L}\right)\left(\frac{\tau}{\tau_+}\right)I_- . \tag{10}$$

The gas within the apparatus was not known precisely, but the slope of this curve yields its average ionization cross section. For $p = 2 \times 10^{-6}$ Torr and a mirror ratio of 5,

$$\sigma_+(?) = 2.4 \times 10^{-17}\ \text{cm}^2.$$

For comparison, the ionization cross section for 1600-volt electrons on CO_2 is

$$\sigma_+(CO_2) = 7.8 \times 10^{-17}\ \text{cm}^2.$$

Since the residual gas in the apparatus is probably composed of heavy molecules, the low ionization cross section indicates approximately 30 per cent collection efficiency.

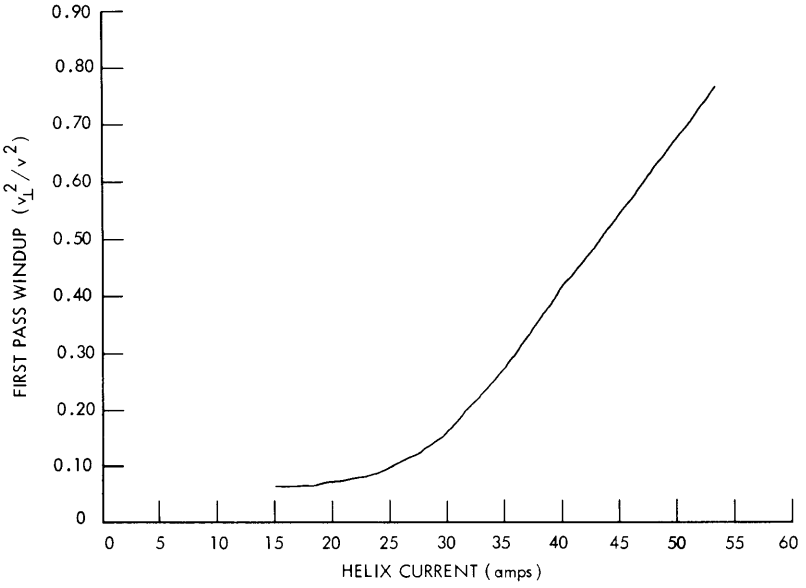

Fig. XVI-9. Calibration curve for ion collector.

Since the corkscrew does not contribute to the trapping, f = 0 in the particle-balance equations. Therefore the dependence of the ratio of ion-to-electron current on pressures as shown in Fig. XVI-10 is given by

$$\frac{I_+}{I_-} = \frac{\tau}{\tau_+}\left(\frac{A_T}{A}\right)\frac{1}{\frac{A_L}{A} + \frac{\tau_g}{\tau_H}} \tag{11}$$

The main pressure dependence is from τ_+, but as the corkscrew is turned on and τ_H decreases from ∞, the slope of the curve in Fig. XVI-10 is seen to change. The ratio

of ion current with the corkscrew off to that with the corkscrew on is given by

$$\frac{I_+(\text{off})}{I_+(\text{on})} = 1 + \frac{A}{A_L}\frac{\tau_g}{\tau_H}. \tag{12}$$

In Fig. XVI-10 the slight downward slope, as pressure is increased, is hidden in the fluctuations caused by the fact that the system pressure could only be varied in a gross manner by blanking off the pumps. The first and last points were the most

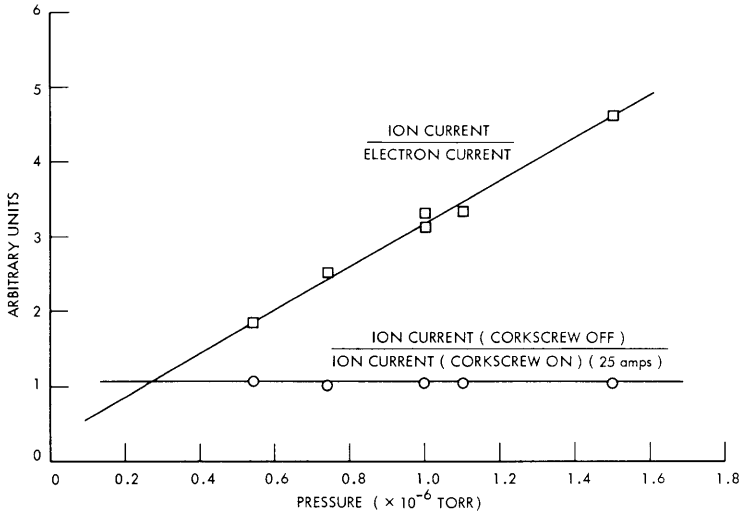

Fig. XVI-10. Pressure variation of ion current.

stable, and they do show a small downward slope of the correct magnitude (~3%). The general agreement between Figs. XVI-9 and XVI-10 and Eqs. 1-6 serves as an indication of the validity of these equations.

In order to study the dissociated-particle interaction, an x-y recorder was used to record the ion current as a function of helix current. Then Eq. 12 was used to obtain the lifetime of particles attributable to the helix scattering as a function of helix current. Figure XVI-11 shows the result plotted on a log-log scale. A power law fits the data over a sevenfold increase in the perturbation strength. At higher currents the ion current saturated because the helix itself began to trap particles. At lower currents the perturbation of the gas scattering was too weak to be seen accurately, but the curve does break away from the law in the direction of longer lifetime, as one would expect.

The surprising aspect of this result is the 3/2 power dependence of the lifetime. The diffusion theories that have been advanced to cover the nonresonant scattering[2, 3] regime led one to expect

$$\tau_H \alpha \left(\frac{B_\perp}{B_o}\right)^{-2} . \qquad (13)$$

The result of this experiment indicates a much faster loss of particles than had been predicted on these earlier theoretical bases. A confirmation of this behavior by another diagnostic technique is clearly required to determine the origin of this enhanced loss.

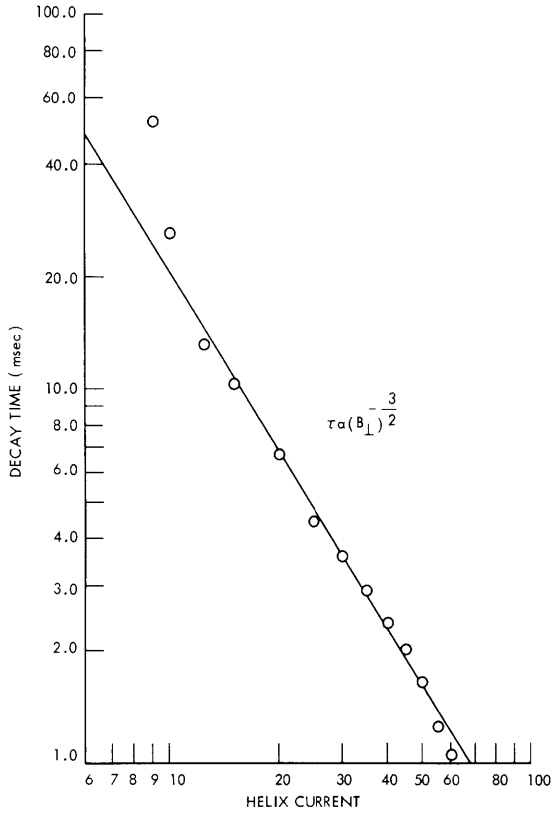

Fig. XVI-11. Lifetime of "dissociated" electrons.

J. F. Clarke

References

1. J. F. Clarke and L. M. Lidsky, Quarterly Progress Report No. 81, Research Laboratory of Electronics, M.I.T., April 15, 1966, pp. 147-159.
2. J. F. Clarke, Quarterly Progress Report No. 79, Research Laboratory of Electronics, M.I.T., October 15, 1965, p. 141.
3. R. C. Wingerson, T. H. Dupree, and D. J. Rose, Phys. Fluids 7, 1475 (1964).
4. E. W. Laing and A. E. Robson, J. Nucl. Energy (Part C, Plasma Physics) 3, 146 (1963).